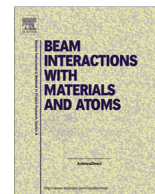




Contents lists available at ScienceDirect

## Nuclear Instruments and Methods in Physics Research B

journal homepage: [www.elsevier.com/locate/nimb](http://www.elsevier.com/locate/nimb)

## Temperature of thermal spikes induced by swift heavy ions

S. Matsuzaki<sup>a</sup>, H. Hayashi<sup>a</sup>, K. Nakajima<sup>a</sup>, M. Matsuda<sup>b</sup>, M. Sataka<sup>b</sup>, M. Tsujimoto<sup>c</sup>, M. Toulemonde<sup>d</sup>, K. Kimura<sup>a,\*</sup><sup>a</sup> Department of Micro Engineering, Kyoto University, Kyoto 615-8540, Japan<sup>b</sup> Nuclear Science Research Institute, JAEA, Tokai, Naka, Ibaraki 319-1195, Japan<sup>c</sup> Institute for Integrated Cell-Material Sciences, Kyoto University, Kyoto 606-8501, Japan<sup>d</sup> CIMAP-GANIL (CEA-CNRS-ENSICAEN-Université de Caen Basse Normandie), Bd. H. Becquerel, 14070 Caen, France

## ARTICLE INFO

## Article history:

Received 1 August 2016

Received in revised form 1 December 2016

Accepted 8 December 2016

Available online xxxxx

## Keywords:

Inelastic thermal spike

Temperature measurement

Swift heavy ion

## ABSTRACT

Few-nm sized gold, platinum and palladium nanoparticles were deposited on amorphous silicon nitride films. These films were irradiated with 420 MeV Au and 100 MeV Xe ions. Temperature distributions of thermal spikes produced by these ions were evaluated by observing desorption of the nanoparticles from the target surfaces upon ion impact. It was found that the temperature of the thermal spike produced by 420 MeV Au is higher than 100 MeV Xe. The observed temperature of the thermal spike at the entrance surface is slightly lower than that at the exit surface both for 420 MeV Au and 100 MeV Xe ions. These results can be well explained by the inelastic thermal spike model.

© 2016 Elsevier B.V. All rights reserved.

## 1. Introduction

Recently we have observed desorption of gold nanoparticles from surfaces of amorphous silicon nitride (a-SiN) and amorphous silicon oxide (a-SiO<sub>2</sub>) upon impact of 420 MeV Au ions [1]. The gold nanoparticles were desorbed as liquid droplet without fragmentation and the desorption occurs in the vicinity (~several nm) of the ion impact position. The mechanism of the observed desorption was ascribed to a so-called popcorn mechanism [2]. When nanoparticles are heated beyond their melting point in a short time period a sudden volume expansion occurs upon melting of nanoparticles. As a result, a large compressive pressure will build up in the nanoparticle. If this pressure is high at the substrate–nanoparticle interface, it will accelerate the nanoparticle away from the surface, leading to desorption. Actually, molecular dynamics (MD) simulations showed that gold nanoparticles are desorbed as liquid droplets from a surface when they are energized beyond 0.4 eV/atom [3]. This threshold energy (0.4 eV/atom) is close to, but slightly smaller than, the energy to reach the melting temperature of gold (1338 K = 0.346 eV/atom) plus the latent heat (0.132 eV/atom) of melting. This was attributed to the size effect on the melting temperature. Thus, the observed nanoparticle-cleared region corresponds to the region where the temperature

surpassed 0.4 eV/atom during the evolution of the thermal spike. This allows us to trace the temperature of thermal spikes. The feasibility of this new temperature tracing method was already examined by comparing the observed radius of the gold-nanoparticle-cleared region with the theoretical calculation using the inelastic thermal spike (i-TS) model [1]. In the present work, we extend our previous work. We measure detailed temperature distributions of thermal spikes using nanoparticles of different materials which have different melting temperatures. We observe desorption of gold, platinum and palladium nanoparticles upon irradiation of 100 MeV Xe and 420 MeV Au ions on a-SiN films. The derived temperature distributions are compared with the results of the i-TS calculations.

## 2. Experimental

Self-supporting a-SiN films of 30 nm thickness (nominal density 3 g/cm<sup>3</sup>) prepared by chemical vapor deposition were purchased from Silson Ltd. The composition of the a-SiN film was determined to be Si<sub>0.47 ± 0.02</sub>N<sub>0.53 ± 0.02</sub> using high-resolution Rutherford backscattering spectrometry [4]. Gold, platinum or palladium nanoparticles were deposited on each a-SiN film by vacuum evaporation. The prepared nanoparticle-deposited films were irradiated with 100 MeV Xe and 420 MeV Au ions at normal incidence to a fluence of ~5 × 10<sup>10</sup> ions/cm<sup>2</sup> at the tandem accelerator facility of Japan Atomic Energy Agency (JAEA). A carbon foil of 20 μg/cm<sup>2</sup> was placed in front of the sample to acquire an equilibrium charge

\* Corresponding author.

E-mail address: [kimura@kues.kyoto-u.ac.jp](mailto:kimura@kues.kyoto-u.ac.jp) (K. Kimura).

state. The irradiation was performed either on the nanoparticle-deposited surface (front surface irradiation) or on the rear surface (rear surface irradiation). The samples were observed using TEM (JEOL JEM-2200FS) equipped with a field emission gun operating at 200 kV. The temperatures of both the entrance and exit surfaces were evaluated by observing desorption of nanoparticles for the front and rear surface irradiations, respectively.

### 3. Results and discussion

Fig. 1(a) shows an example of the TEM bright field images of the Pt-deposited a-SiN film observed before irradiation. There are many platinum nanoparticles formed by the vapor deposition. The areal density,  $N$ , of these nanoparticles was measured to be  $9.5 \times 10^{12}$  particles/cm<sup>2</sup>. The size distribution of these nanoparticles was derived from the observed TEM images. The distribution shows a Gaussian-like well-defined peak with a peak diameter of 1.5 nm and FWHM of 0.95 nm. Similar size distributions were also observed for Pd and Au nanoparticles with peak diameters of 2 and 4 nm, respectively.

Fig. 1(b) shows an example of TEM bright field images of the Pt-deposited a-SiN film observed after irradiation with 100 MeV Xe ions on the rear surface. Ion tracks are seen as small bright spots. It is seen that the Pt nanoparticles disappeared from the surrounding area of the ion tracks. Such disappearance of the nanoparticles was also observed when the sample was irradiated on the front surface. It is noteworthy that the size of the ion track (diameter  $\sim 1$  nm) produced by the 100 MeV Xe ion is close to the detection limit of TEM. Thus, some of the ion tracks produced by 100 MeV Xe ions might not be observed by the present TEM observation.

The distance,  $R$ , between the ion track and the closest nanoparticle was measured for each ion track. The distributions of  $R$  for the Pt-deposited a-SiN irradiated with 100 MeV Xe ions are shown by closed circles in Fig. 2. The distribution shows a Gaussian-like well-defined peak with a peak radius of 5.2 nm. Similar analyses were also performed for the rear surface irradiations of Pd- and Au-deposited a-SiN films. The derived  $R$ -distributions are shown by triangles (Pd-deposited film) and squares (Au-deposited film) in Fig. 2. These distributions also show a Gaussian-like well-defined peak with a peak radius of 7.4 and 9.2 nm for Pd- and Au-deposited a-SiN films, respectively. These results indicate that the nanoparticle-cleared region increases with decreasing melting temperature (2045, 1828 and 1338 K for Pt, Pd and Au) Because the temperature of the thermal spike decreases with increasing dis-

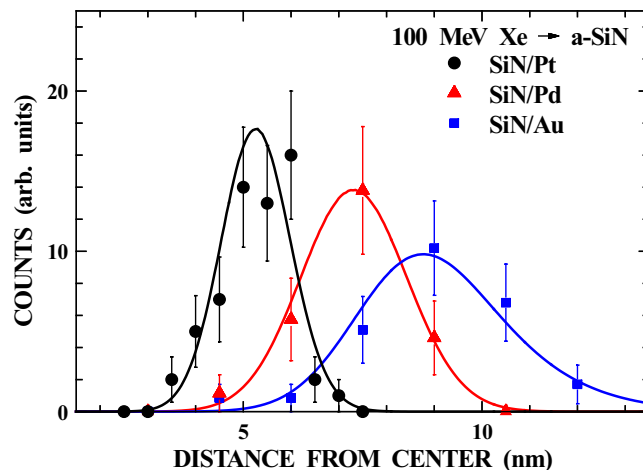


Fig. 2. Distributions of the distance between the ion track and the closest nanoparticle observed after irradiation of 100 MeV Xe ions on the rear surface of a-SiN film. The result of Pt, Pd and Au nanoparticles are shown by circles, triangles and squares, respectively. The theoretical distributions (Eq. (1)) convoluted with a Gaussian function are shown by solid lines.

tance from the track center, this is consistent with the finding by the MD simulation that nanoparticles are desorbed when they are heated beyond their melting point.

Although the measured  $R$  represents the radius of nanoparticle-cleared region ( $R_c$ ) it is not exactly equal to  $R_c$ . According to the Poisson law, the  $R$ -distribution is given by [1]

$$P(R)dR = \begin{cases} 2\pi RN \exp\{-N\pi(R^2 - R_c^2)\}dR & \text{for } R > R_c, \\ = 0 & \text{for } R \leq R_c, \end{cases} \quad (1)$$

where we assumed that the desorption probability is 100% in the region  $r < R_c$  and 0% in the region  $r > R_c$  ( $r$  denotes the distance from the track center). The average of the closest distance can be calculated by

$$\langle R \rangle = \int_0^\infty P(R)RdR = R_c + \frac{\exp(\pi NR_c^2)}{2\sqrt{N}} \operatorname{erfc}(\sqrt{\pi NR_c}). \quad (2)$$

Substituting the observed  $\langle R \rangle$  and  $N$  into Eq. (2),  $R_c$  can be determined. The obtained nanoparticle cleared radii are  $R_c = 5.0 \pm 0.6$ ,  $6.9 \pm 0.8$  and  $7.6 \pm 1.1$  nm for Pt-, Pd- and Au-nanoparticles, respectively. The  $R$ -distributions [Eq. (1)] were cal-

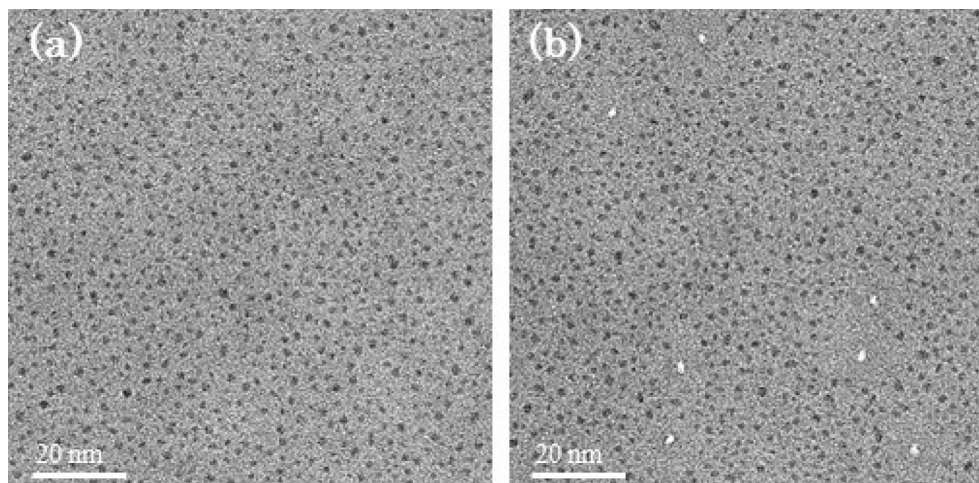


Fig. 1. TEM bright field images of Pt-deposited 30-nm a-SiN films. The images observed (a) before and (b) after irradiation with 100 MeV Xe ions on the rear surface are shown. The ion tracks are seen as small bright spots. The platinum nanoparticles disappeared from the vicinity of the ion track after irradiation.

Download English Version:

<https://daneshyari.com/en/article/5467557>

Download Persian Version:

<https://daneshyari.com/article/5467557>

[Daneshyari.com](https://daneshyari.com)